Voltage-gated Transient Currents in Bovine Adrenal Fasciculata Cells

I. T-type Ca^{2+} Current

BORIS MLINAR, BRUCE A. BIAGI, and JOHN J. ENYEART

From the Department of Pharmacology and the Neuroscience Program, and Department of Physiology, Ohio State University, Columbus, Ohio 43210-1239

ABSTRACT The whole cell version of the patch clamp technique was used to identify and characterize voltage-gated Ca^{2+} channels in enzymatically dissociated bovine adrenal zona fasciculata (AZF) cells. The great majority of cells (84 of 86) expressed only low voltage–activated, rapidly inactivating Ca^{2+} current with properties of T-type Ca^{2+} current described in other cells. Voltage-dependent activation of this current was fit by a Boltzmann function raised to an integer power of 4 with a midpoint at −17 mV. Independent estimates of the single channel gating charge obtained from the activation curve and using the "limiting logarithmic potential sensitivity" were 8.1 and 6.8 elementary charges, respectively. Inactivation was a steep function of voltage with a $v_{1/2}$ of −49.9 mV and a slope factor K of 3.73 mV. The expression of a single Ca^{2+} channel subtype by AZF cells allowed the voltage-dependent gating and kinetic properties of T current to be studied over a wide range of potentials. Analysis of the gating kinetics of this Ca^{2+} current indicate that T channel activation, inactivation, deactivation (closing), and reactivation (recovery from inactivation) each include voltage-independent transitions that become rate limiting at extreme voltages. Ca^{2+} current activated with voltage-dependent sigmoidal kinetics that were described by an m^4 model. The activation time constant varied exponentially at test potentials between −30 and +10 mV, approaching a voltage-independent minimum of 1.6 ms. The inactivation time constant (τ_i) also decreased exponentially to a minimum of 18.3 ms at potentials positive to 0 mV. T channel closing (deactivation) was faster at more negative voltages; the deactivation time constant (τ_d) decreased from 8.14 ± 0.7 to 0.48 ± 0.1 ms at potentials between −40 and −150 mV. T channels inactivated by depolarization returned to the closed state along pathways that included two voltage-dependent time constants. $\tau_{rec\text{-}s}$ ranged from 8.11 to 4.80 s when the recovery potential was varied from −50 to −90 mV, while $\tau_{rec\text{-}f}$ decreased from 1.01 to 0.372 s. At potentials negative to −70 mV, both time constants approached minimum values. The low voltage–activated Ca^{2+} current in AZF cells was blocked by the T channel selective antagonist Ni^{2+} with an IC_{50} of 20 μM. At similar

Address reprint requests to Dr. John J. Enyeart, Department of Pharmacology, The Ohio State University College of Medicine, Columbus, OH 43210-1239.

J. GEN. PHYSIOL. © The Rockefeller University Press · 0022-1295/93/08/0217/21 $2.00
Volume 102 August 1993 217–237

concentrations, Ni^{2+} also blocked cortisol secretion stimulated by adrenocorticotropic hormone. Our results indicate that bovine AZF cells are distinctive among secretory cells in expressing primarily or exclusively T-type Ca^{2+} channels. These channels serve as the major pathway for voltage-gated Ca^{2+} entry and may mediate peptide hormone–stimulated cortisol secretion in these cells.

INTRODUCTION

In mammals, cortisol secretion by cells from the fasciculata of the adrenal cortex occurs in a diurnal pattern under the control of the pituitary peptide hormone adrenocorticotropic hormone (ACTH). In addition to the basal rhythmic secretory pattern, physical and psychological stress can evoke major episodic bursts of secretion (Bondy, 1985). The cellular, biochemical, and electrophysiological mechanisms that function in the regulation of cortisol synthesis and secretion are not well understood. In particular, the role of electrical activity and specific ion channels in cortisol production is unknown.

In many secretory cells, voltage-gated Ca^{2+} channels couple electrical activity to the secretion of transmitters and hormones. Ca^{2+} flux studies have suggested that voltage-gated Ca^{2+} channels participate in the regulation of cortisol synthesis by bovine adrenal zona fasciculata (AZF) cells (Yanagibashi, Kawamura, and Hall, 1990). Although several types of voltage-gated Ca^{2+} channels have been identified in rat and bovine adrenal glomerulosa cells (Cohen and McCarthy, 1987; Matsunaga, Maruyama, Kojima, and Hoshi, 1987; Durroux, Gallo-Payet, and Payet, 1988), Ca^{2+} channels in AZF cells have not been studied with voltage clamp methods. Identification and characterization of membrane Ca^{2+} currents in AZF cells will be a necessary step toward understanding the function of Ca^{2+} channels in the physiological regulation of cortisol synthesis.

Based on differences in biophysical properties and pharmacology, at least four types of voltage-gated Ca^{2+} channels have been identified in excitable cells (Bean, 1989; Hess, 1990). Two of these channels may be specific to neurons, while L- and T-type Ca^{2+} channels have been found in a wide range of cells. High voltage–activated L-type Ca^{2+} channels inactivate slowly and permit large quantities of Ca^{2+} to enter a depolarized cell. They are sensitive to the major organic Ca^{2+} antagonists. Low voltage–activated, rapidly inactivating T-type Ca^{2+} channels coexist with L-type channels in many excitable cells, including endocrine secretory cells (Bean, 1989; Hess, 1990). T channels appear to function in regulating action potential generation in spontaneously active cells (Armstrong and Matteson, 1985; Suzuki and Rogawski, 1989; Wang, Rinzel, and Rogawski, 1991), but Ca^{2+} entering through T channels may also serve as an intracellular messenger (Enyeart, Biagi, Day, Sheu, and Mauer, 1990). The presence of multiple Ca^{2+} channels in most excitable cells has hindered the study of individual subtypes with respect to biophysical properties and role in cellular function.

In this study we used the whole cell version of the patch clamp technique to describe voltage-gated Ca^{2+} channels in enzymatically dissociated bovine AZF cells. Nearly every cell expressed only a low voltage–activated T-type Ca^{2+} current. The presence of a single Ca^{2+} channel subtype in these nearly spherical cells provided an

unusual opportunity for a comprehensive characterization of the biophysical properties of this current.

MATERIALS AND METHODS

Materials

Tissue culture media, antibiotics, fibronectin, and fetal calf serum were obtained from GIBCO BRL (Gaithersburg, MD). Culture dishes were purchased from Corning Inc. (Corning, NY). Coverslips were from Bellco Biotechnology (Vineland, NJ). Enzymes, ACTH (1–24), tetrodotoxin, GTP, MgATP, isobutylmethylxanthine, forskolin, $NiCl_2$, and $LaCl_3$ were obtained from Sigma Chemical Co. (St. Louis, MO). YCl_3 (99.9% purity) was obtained from Aldrich Chemical Co. (Milwaukee, WI). The dihydropyridine (-)Bay K 8644 was kindly donated by Alexander Scriabine, Miles Institute of Preclinical Pharmacology (West Haven, CT). ω-Conotoxin was purchased from Peninsula Laboratories, Inc. (Belmont, CA).

Methods

Isolation and culture of AZF cells. Bovine adrenal glands were obtained from steers (age range 1–3 yr) within 15 min of slaughter at a local slaughterhouse. Fatty tissue was removed immediately and the glands were transported to the laboratory in ice-cold PBS containing 0.2% dextrose. Isolated AZF cells were prepared as previously described (Gospodarowicz, Ill, Hornsby, and Gill, 1977) with some modifications. In a sterile tissue culture hood, the adrenals were cut in half lengthwise and the lighter medulla tissue was trimmed away from the cortex and discarded. The capsule with attached glomerulosa and thicker fasciculata–reticularis layer were then dissected into pieces ~1.0 × 1.0 × 0.5 cm. A Stadie-Riggs tissue slicer (Thomas Scientific, Swedesboro, NJ) was used to slice fasciculata–reticularis tissue from the glomerulosa layers. Fasciculata–reticularis slices were diced into 0.5-mm^3 pieces and dissociated with 2 mg/ml (~200 U/ml) of type I collagenase and 0.2 mg/ml deoxyribonuclease in MEM plus 100 U/ml penicillin and 0.1 mg/ml streptomycin for ~45 min at 37°C in a shaking water bath, triturating after 15 and 30 min with a sterile, plastic transfer pipette. After incubating, the suspension was filtered through one layer of sterile cheesecloth and centrifuged to pellet cells at 100 *g* for 5 min. The cells were then washed twice with MEM, centrifuging as before to pellet. Cells were filtered through 200-μm stainless steel mesh to remove clumps after resuspending in MEM. Dispersed cells were again centrifuged and either resuspended in DMEM/F12 (1:1) with 10% FBS, 100 U/ml penicillin, 0.1 mg/ml streptomycin, and the antioxidants tocopherol (1 μM), selenite (20 nM), and ascorbic acid (100 μM) and plated for immediate use, or resuspended in FBS/5% DMSO and stored in liquid nitrogen for future use. Cells were plated in 35-mm dishes containing 9-mm^2 glass coverslips that had been treated with fibronectin (10 μg/ml) at 37°C for 30 min and then rinsed twice with warm, sterile PBS immediately before adding cells. Dishes were maintained at 37°C in a humidified atmosphere of 95% air and 5% CO_2.

Solutions and recording conditions. Solutions for patch clamp experiments were designed to eliminate K^+ currents and minimize Ca^{2+} channel washout. The standard intracellular solution was 120 mM CsCl, 1 mM $CaCl_2$, 2 mM $MgCl_2$, 11 mM BAPTA, 10 mM HEPES, and 1 mM MgATP with pH titrated to 7.2 using CsOH. The external solution consisted of 117 mM TEACl, 5 mM CsCl, 10 mM $CaCl_2$, 2 mM $MgCl_2$, 5 mM HEPES, and 5 mM glucose, with pH adjusted to 7.4 using TEAOH. Deviations from these solutions are noted in the text. All solutions were filtered through 0.22-μm cellulose acetate filters.

AZF cells were used for patch clamp experiments 2–48 h after plating. Typically, cells with diameters of 15–30 μm and capacitances of 15–35 pF were selected. Coverslips were

transferred from 35-mm culture dishes to the recording chamber (volume, 1.5 ml), which was continuously perfused by gravity at a rate of 4–6 ml/min. Patch electrodes with resistances of 1.0–2.0 MΩ were fabricated from Corning RC-6 or 0010 glass (Garner Glass Co., Claremont, CA). Whole cell currents were recorded at room temperature (22–24°C) following the procedure of Hamill, Marty, Neher, Sakmann, and Sigworth (1981) using an EPC-7 patch clamp amplifier (List Biological Laboratories Inc., Campbell, CA).

Pulse generation and data acquisition were done using an IBM-AT computer and PCLAMP software with an Axolab interface (Axon Instruments, Inc., Foster City, CA). Currents were digitized at 1–50 kHz after filtering with an 8-pole Bessel filter (Frequency Devices Inc., Haverhill, MA). Linear leak and capacity currents were subtracted from current records using scaled hyperpolarizing steps of ½ to ¼ amplitude. Data were analyzed and plotted using PCLAMP (CLAMPAN and CLAMPFIT) and GraphPAD InPLOT.

Series resistance compensation was not utilized in most experiments. By using low-resistance electrodes (<2 MΩ) which typically gave access resistances of <5 MΩ and selecting small cells of <20 pF, the time constant of our voltage clamp was typically <100 μs. Exponential fits of whole cell currents and tails were begun only after a period of four time constants. The mean amplitude of T-type Ca^{2+} current in AZF cells was <300 pA. A current of this size in combination with 5 MΩ access resistance produces a voltage error of only 1.5 mV, which was not corrected. Amplitude of larger tail currents were determined by extrapolating the fitted single exponential back to time zero beginning from a point where the estimated voltage error was <3 mV. The 1-pole RC filter produced by the combination of series resistance and membrane capacitance would not significantly attenuate transients with frequencies <5 kHz in our recordings.

Drugs were applied by bath perfusion controlled manually by a six-way rotary valve. Dihydropyridines and penfluridol were dissolved in ethanol and diluted into test solutions. The final ethanol concentration never exceeded 0.05%, which by itself did not affect Ca^{2+} current.

RESULTS

Initial whole cell patch clamp studies indicated that, unlike most secretory cells, AZF cells do not express TTX-sensitive Na^+ currents. Rather, the sole inward current detectable in the great majority of cells is a low voltage–activated Ca^{2+} current. When depolarizing steps were applied from a holding potential of −80 mV, Ca^{2+} currents were detected at test potentials positive to −50 mV and reached a maximum amplitude between −20 and −10 mV (Fig. 1). At test voltages positive to −30 mV, the leak-subtracted current decayed within 200 ms to a value indistinguishable from zero. When test potentials were applied from a holding potential of −40 mV, this current component was not available for activation. A slowly inactivating L-type Ca^{2+} current could be activated from −40 mV in only 2 of 86 cells tested. The results indicate that the major Ca^{2+} current expressed by cells of the bovine AZF is similar to T-type currents previously described in other cells.

The magnitude of the Ca^{2+} current varied linearly with cell size as determined from cell capacitance measurements. For 38 cells, the maximum Ca^{2+} current averaged 272 ± 25.3 pA. When peak membrane current was plotted as a function of cell capacitance for these 38 cells, a least-squares linear regression analysis yielded a line with a slope of 8.2 ± 1.4 pA/pF. When the ratio of current to capacitance was plotted as a function of capacitance for the same 38 cells, the least-squares linear regression yielded a line with a slope not different from zero and an intercept of 8.93 ± 1.49 pA/pF, indicating that T channel density did not vary with cell size (data not shown).

Conductance of Open Channels

The instantaneous current–voltage relationship (IIV) is a measure of the voltage-dependent conducting properties of open ion channels. IIV curves for T current in AZF cells were obtained by two separate protocols (Fenwick, Marty, and Neher, 1982). In the first of these, Ca^{2+} channels were opened by a brief (5–10 ms)

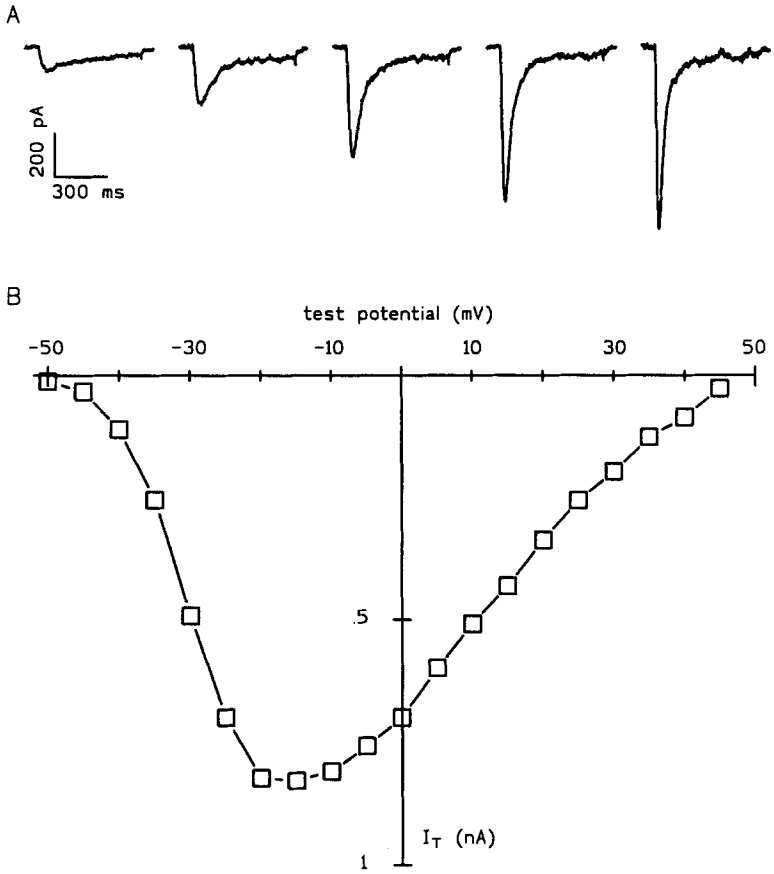

FIGURE 1. Low voltage–activated Ca^{2+} currents in bovine AZF cells. Whole cell Ca^{2+} currents were activated by voltage steps to various test potentials applied at 0.1 Hz from a holding potential of −80 mV. (*A*) Current traces recorded at the indicated test voltages. (*B*) Current–voltage relationship; peak current amplitudes are plotted as a function of test potential. Cell 1O03#1.

depolarizing step to 0 mV, after which the membrane potential was stepped down to a new value between −30 and −150 mV where the current was measured, before a change in the number of open channels theoretically occurred. Alternatively, for voltages from −30 to +80 where tail currents were small, the IIV was determined by applying test pulses over this range and measuring the current immediately upon returning to a single holding potential (−80 mV). The ratio of the Ca^{2+} current

amplitude at the end of the pulse and peak tail current amplitude were plotted against the test potential to give the IIV relationship. Peak tail current amplitudes were determined by extrapolating exponential fits back to the time of repolarization. The data from the two methods were made comparable by an appropriate scaling factor derived from values at 0 mV.

Under the conditions of our experiment (a 10^6-fold asymmetry in Ca^{2+} concentration between the pipette and external solutions), a highly nonlinear IIV relationship marked by downward negative curvature was observed (Fig. 2 *A*). Over a wide range of potentials (−80 to +30 mV), the IIV relationship was well described by the Goldman-Hodgkin-Katz constant field expression (Goldman, 1943; Hodgkin and Katz, 1949) (Fig. 2 *B*). At more positive potentials, inward current was smaller than predicted and crossed the voltage axis at potentials more negative than E_{ca}. At potentials progressively more negative than −80 mV, inward current increased dramatically over that predicted by the constant field equation (Fig. 2 *A*).

Voltage-dependent Steady-State Activation and Inactivation

The voltage dependence of T current activation was determined by dividing peak current amplitudes from the steady-state IV relationships by corresponding current amplitudes from the IIV. The fraction of open channels was then plotted against membrane potential and fit by a Boltzmann function of the form: fraction open = $1/[1 + \exp(v_{1/2} - v)/K]^N$, where $v_{1/2}$ is the voltage at which half of the single-gate sensors are in the open conformation, K is the slope factor, and N is an integer number of single-gate voltage sensors or conformational states associated with the opening of one channel. Activation curves for $N = 4$ (solid line), which gave the best fit, and $N = 1$ (dotted line) are shown in Fig. 3 *A*. The M_∞ curve which describes the activation function of one of four independent voltage sensors has a $v_{1/2}$ of −36.5 mV and a K of 11.8 mV per e-fold change. A slope factor of 11.8 mV combined with an N value of 4 is consistent with a model where the opening of a single T-type Ca^{2+} channel is associated with the movement of 8.1 elementary charges through the entire electric field of the membrane.

A model-independent estimate of the single channel gating charge was obtained using the limiting logarithmic potential sensitivity of channel activation (Armstrong and Eckert, 1987; Schoppa, McCormack, Tanoute, and Sigworth, 1992). Values from the activation curve can be used to determine the ratio of opened to closed channels as a function of voltage. For channels obeying a Boltzmann equilibrium law, an expression relating the fraction of open channels to membrane voltage is given by: $d(\ln O/C)/dV = q/kT$, where O/C is the ratio of open to closed Ca^{2+} channels, q is the single channel gating charge, k is the Boltzmann constant, and T is the temperature. At negative potentials where the fraction of open channels is small, the logarithmic potential sensitivity provides an estimate of the minimum charge displacement (q) required for the opening of a single Ca^{2+} channel. The logarithmic potential sensitivity was determined from activation curves for nine cells (Fig. 3 *B*). A semilogarithmic plot of the ratio of open to closed channels as a function of membrane potential provided a curve that was nearly linear at negative voltages (−50

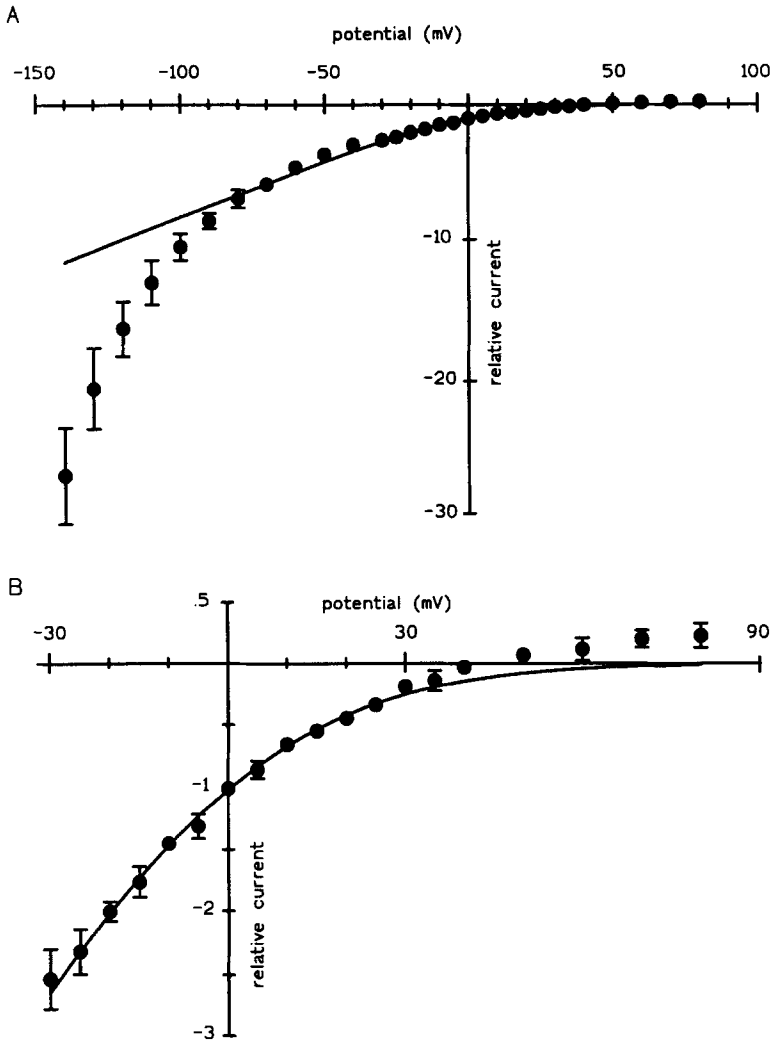

FIGURE 2. Open channel current–voltage relationship for T-type Ca^{2+} channel. IV relationships for open channels were obtained using two separate methods. In the first, T channels were activated by 5-ms test pulses to 0 mV. Currents were then measured after stepping to various voltages between −140 and −40 mV. In the second method (used for points positive to −40 mV), Ca^{2+} currents were activated by depolarizing steps to potentials ranging from −30 to +80 mV, after which membrane potential was returned to the holding potential of −80 mV where decaying tail currents were measured. The ratio of the Ca^{2+} current at the end of the pulse to the peak tail current was plotted as a function of the test voltage for potentials from −30 to +80 mV to give the open channel IV. Relative currents are plotted against test potential for voltages from −140 to +80 mV (*A*) and −30 to +80 mV (*B*). Instantaneous IV predicted from Goldman-Hodgkin-Katz constant field expression. Values are mean ± SEM of four to eight independent measurements.

to −40 mV), with a slope (q/KT) corresponding to an e-fold increase per 3.53 mV change in membrane voltage (Fig. 3 *B*, solid line). This limiting logarithmic potential sensitivity corresponds to a single channel gating charge q of 6.8 e.

The voltage-dependent steady-state inactivation of the low voltage–activated Ca^{2+} current was studied by applying 10-s conditioning pulses to various potentials,

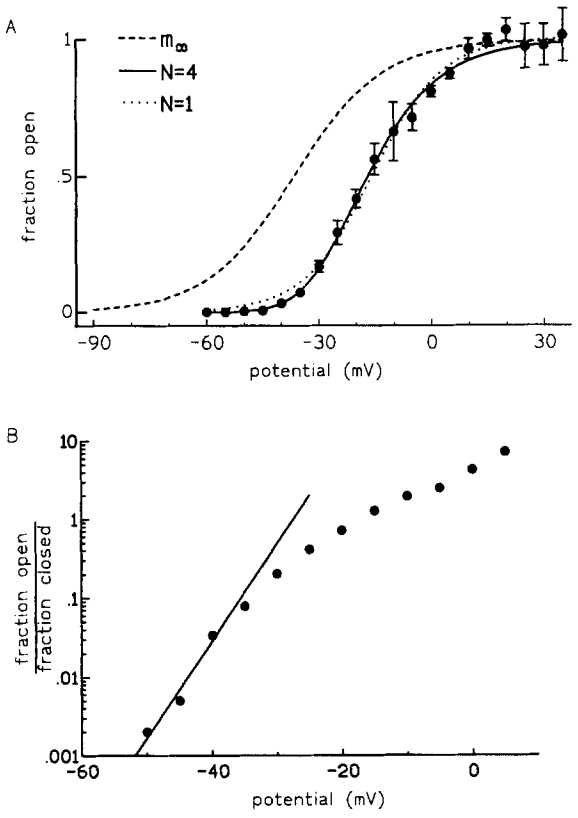

FIGURE 3. Voltage dependence of T channel opening and associated gating charge. (*A*) Voltage-dependent activation of T current was determined by dividing peak current amplitudes obtained from steady-state IV relationships by corresponding current amplitudes from the open channel IV relationship obtained as described in the legend of Fig. 2. These values were normalized to the maximum permeability. The normalized values representing the fraction of open channels were plotted against membrane potential to give the activation function. Data were fit by Boltzmann functions of the form: fraction open = $1/[1 + \exp(v_{1/2} - v)/K]^N$. Activation curves for $N = 4$ (*solid line*) and $N = 1$ (*dotted line*) are shown. M_∞ curve corresponding to $N = 4$ has a $v_{1/2}$ of −36.5 mV and a slope factor of 11.8 mV/e-fold change. Values are mean ± SEM of five to eight independent measurements. (*B*) Limiting logarithmic potential sensitivity. The ratio of open to closed T-type Ca^{2+} channels was determined from steady-state activation curves for nine cells. The logarithm of this ratio was plotted against membrane potential and the slope computed at potentials between −50 and −40 mV. The slope of the curve, an e-fold increase per 3.53 mV at the most negative potentials (*solid line*), is the logarithmic potential sensitivity, corresponding to a single channel gating charge of 6.8 e.

followed by activating voltage steps to −10 mV. The normalized current was plotted as a function of conditioning voltage and fitted with the equation: $I/I_{max} = 1/[1 + \exp(v - v_{1/2})/K]$, where I_{max} was the current activated from a holding potential of −90 mV. Inactivation was a steep function of voltage with $v_{1/2}$ equal to −49.9 mV and a slope factor K of 3.73 mV per e-fold change (Fig. 4, solid line).

Voltage-dependent Gating Kinetics

The expression of only T-type Ca^{2+} current by AZF cells provided a unique opportunity to study, over a wide range of potentials, their voltage-dependent gating kinetics, including activation, inactivation, deactivation, and recovery from inactivation. The activation kinetics of T-type current were voltage dependent and marked by a clear delay in the rising phase of the current. To describe the sigmoidal current, onset traces taken from IV protocols were fit with the following equation: $I_{Ca} = I_\infty [1 - \exp(T/\tau_a)]^N \exp(-T/\tau_i)$, where τ_a and τ_i are activation and inactivation time constants, N is an integer between 1 and 4, and I_∞ is the current that would be reached in the absence of inactivation. Best fits were obtained with $N = 4$. Integer values of less than 4 produced too little delay in activation, especially at more positive test potentials.

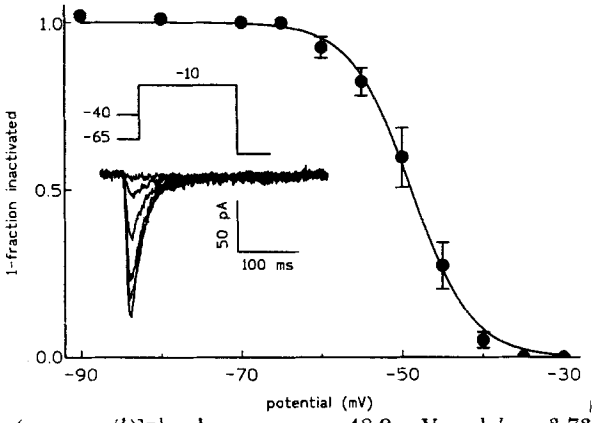

FIGURE 4. Voltage-dependent inactivation. Currents were activated by test pulses to −10 mV after 10-s conditioning pulses to various potentials between −90 and −30 mV. Peak current amplitudes normalized to the maximum current obtained at −90 mV were plotted against conditioning voltage. Mean values ± SE ($n = 4$ cells) were fitted with a smooth curve according to the Boltzmann relationship, $I/I_{max} = [1 + \exp(v - v_{1/2}/k)]^{-1}$, where $v_{1/2} = -48.9$ mV and $k = 3.73$ mV. (*Inset*) T-type Ca^{2+} current records showing inactivation at prepulse potentials of −65 to −40 mV. Cell 1O24#4.

The onset of Ca^{2+} current activation was faster with stronger depolarizations. The activation time constant (τ_a) varied from 8.2 to 2.8 ms at test potentials of −30 and +10 mV, respectively. The relationship between τ_a and membrane voltage could be fit with a single exponential with an e-fold change per 46 mV in test potential, and a voltage-independent offset of 1.6 ms (Fig. 5*A*). The failure of τ_a to decrease exponentially to 0 suggests that voltage-independent transitions exist in the pathway from the closed to the open state.

A distinctive feature of T-type Ca^{2+} currents is their transient waveform during voltage clamp steps as channels move among closed, open, and inactivated states. In some cells, the rate of T current inactivation (τ_i) is voltage dependent over a range of potentials but appears to approach a voltage-independent minimum at more positive voltages (Chen and Hess, 1990). However, accurate measurements of τ_i at positive potentials are limited in most excitable cells by the presence of one or more high voltage–activated Ca^{2+} channels. We measured T Ca^{2+} current inactivation kinetics at test voltages ranging from −40 to +40 mV using both Ca^{2+} and Ba^{2+} as the charge

carrier. With 10 mM Ca^{2+} as the charge carrier, individual decaying currents could be fit with single exponential functions over the entire range of voltages. For test potentials ranging from −40 to 0 mV, τ_i decreased as a smooth function of voltage. With stronger depolarizations, a clear voltage-independent minimum was achieved (Fig. 5 *B*). The relationship expressing τ_i as a function of voltage could be fit with a

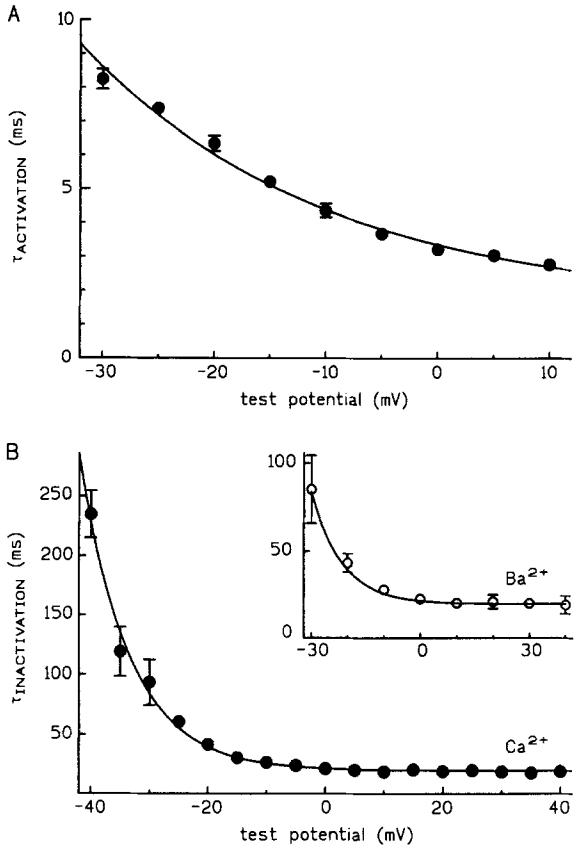

FIGURE 5. Voltage dependence of Ca^{2+} current activation and inactivation kinetics. (*A*) Activation: Currents were activated by test pulses to various test potentials from a holding potential of −80 mV. Current traces were fit with exponential functions of the $m^x h$ form with integer values of x from 1 to 4. Best fits were obtained by the $m^4 h$ model. Activation time constants (mean ± SEM) obtained at various potentials for five to seven different cells were plotted as a function of test voltage. The smooth line indicates approximately exponential voltage dependence of τ_a, with *e*-fold changes per 46 mV and a voltage-independent offset of 1.6 ms. (*B*) Inactivation: Current through T-type Ca^{2+} channels was activated by voltage steps of varying size from a holding potential of −80 mV with either 10 mM Ca^{2+} or Ba^{2+} as the charge carrier. Inactivation time constants (τ_i) were determined at each test potential by fitting the decaying phase of each current with a single exponential. Inactivation time constants were plotted as a function of test potential. Smooth lines indicate approximately exponential voltage dependence of τ_i with *e*-fold change per 10.8 mV and a voltage-independent offset of 18 ms. Points are mean ± SEM from 3–17 separate determinations. (*Inset*) τ_i plotted against membrane potential with Ba^{2+} as the charge carrier.

single exponential with an *e*-fold change per 9.3 mV and a voltage-independent offset of 18.3 ms.

For some Ca^{2+} channel subtypes, the rate and extent of inactivation is reduced when Ba^{2+} replaces Ca^{2+} as the charge carrier. Substitution of Ba^{2+} for Ca^{2+} did not appreciably alter inactivation kinetics of AZF T-type current (Fig. 5 *B*, *inset*). In the presence of 10 mM Ba^{2+}, τ_i was comparable, at each test potential, to that observed

with Ca^{2+} as the charge carrier. Again, at test potentials positive to 0 mV, τ_i approached a clear voltage-independent minimum value of ~18 ms.

Among Ca^{2+} channel subtypes, T-type channels are distinguished by their slow rate of closing. The voltage-dependent kinetics of channel closing in AZF cells was measured as the rate of tail current decay, subsequent to an activating test pulse, at repolarization potentials ranging from −40 to −150 mV. Decaying tail currents (Fig. 6 *A*) could each be fit with a single exponential time constant (τ_d) which decreased smoothly with repolarization voltage. The rate of channel closing was strongly voltage dependent, with τ_d's ranging from 8.14 ± 0.67 ms at −40 mV to 0.48 ± 0.07 ms at −150 mV (Fig. 6 *B*). The function relating τ_d to repolarization potential could be approximated by a single exponential, characterized by an *e*-fold change in τ_d per 32.4 mV and a voltage-independent offset of ~0.27 ms (Fig. 6 *B*). This result suggests that T channel deactivation includes a relatively rapid transition which is intrinsically voltage independent and observable only at extreme potentials, where voltage-dependent rate constants are not rate limiting.

The kinetics of inactivated channels returning to the closed state was studied by voltage clamping cells at −20 mV for 30 s to completely inactivate all Ca^{2+} channels, and then switching to a more negative recovery potential for various periods before applying an activating test pulse to 0 mV (Fig. 7 *A*). The rate of recovery of inactivated channels was clearly voltage dependent at reactivation potentials ranging from −50 to −70 mV. At more negative potentials, recovery reached a voltage-independent maximum rate. In Fig. 7 *B*, the fraction of current recovered is plotted with respect to the duration of reactivating prepulses at −50, −60, and −80 mV as indicated. The recovery curves at −70 and −90 mV have been omitted for clarity, but both were nearly superimposable with the one obtained at −80 mV.

Recovery at each potential occurred by a process with two separate time constants, $\tau_{rec\text{-}s}$ and $\tau_{rec\text{-}f}$; both displayed similar voltage dependence (Fig. 7 *C*). $\tau_{rec\text{-}s}$ ranged from 8.11 to 4.80 s when the recovery potential was varied from −50 to −90 mV. At these same voltages, $\tau_{rec\text{-}f}$ decreased from 1.01 to 0.372 s. Neither time constant changed significantly when recovery was measured at −70, −80, or −90 mV. The fraction of total current recovering with fast kinetics varied slightly with recovery potential decreasing from 0.68 at −50 mV to a voltage-independent minimum of 0.53 at −80 mV (Fig. 7 *D*).

Permeation and Pharmacology

Replacing Ca^{2+} with Ba^{2+} produced very little change in the magnitude or voltage-dependent activation of Ca^{2+} current in AZF cells. Fig. 8 *A* shows averaged and normalized IV curves obtained for seven cells in 10 mM Ca^{2+}, and after switching to external saline containing Ba^{2+}. No significant difference in current was observed at any test potential. Increasing Ca^{2+} from 2 to 5 and finally 10 mM produced less than proportional increases in the magnitude of the peak Ca^{2+} current. In the experiment illustrated in Fig. 8 *B*, when $[Ca^{2+}]_e$ was increased from 2 to 10 mM, the magnitude of the peak Ca^{2+} current increased only twofold.

In most excitable cells, T-type Ca^{2+} channels are resistant to block by the major organic Ca^{2+} antagonists, but are preferentially blocked by Ni^{2+}. Nickel reversibly blocked low voltage–activated Ca^{2+} channels in AZF cells with an IC_{50} of ~20 μM

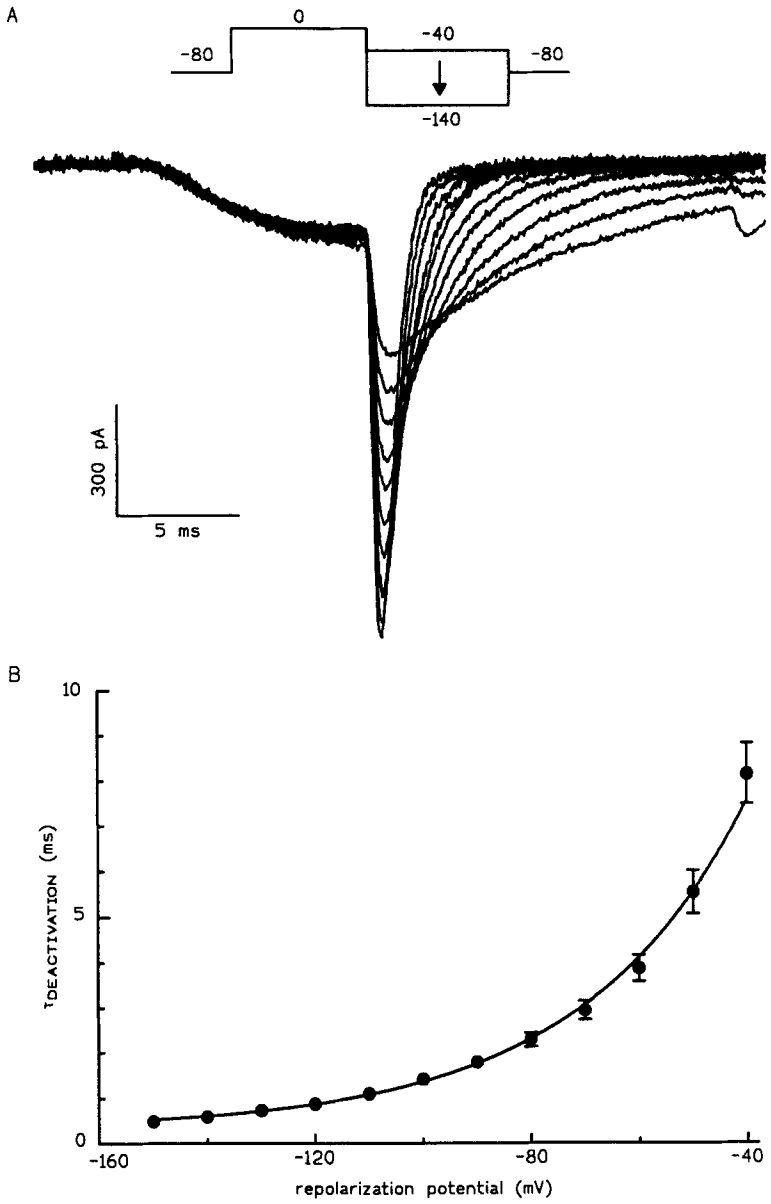

FIGURE 6. Voltage dependence of deactivation kinetics. (*A*) Decaying tail currents were recorded at potentials ranging from −40 to −150 mV after activation by a 10-ms voltage step to 0 mV from a holding potential of −80 mV. Deactivation time constants (τ_d) were determined for each repolarization potential by fitting tail currents with a single exponential function. Cell 1O03#2. (*B*) Deactivation time constants were plotted as a function of repolarization voltage. Smooth line indicates approximately exponential voltage dependence of τ_d, with *e*-fold change per 32.4 mV. Points are mean ± SEM (n = 15 cells).

(n = 4) (Fig. 9). Compared with Ni^{2+}, trivalent lanthanide and nonlanthanide elements were considerably more potent antagonists of T-type Ca^{2+} channels in these adrenal cells. Lanthanum (La^{3+}) blocked the Ca^{2+} current half-maximally at a concentration of 1.5 μM (n = 3). The nonlanthanide trivalent yttrium (Y^{3+}) was the most potent of the inorganic antagonists, with half-maximal inhibition observed at a concentration of 300 nM (n = 3). Inhibition by both La^{3+} and Y^{3+} was reversed upon superfusion of normal saline. Reversal was accelerated by addition of EGTA (0.1 mM) to the perfusate (data not shown).

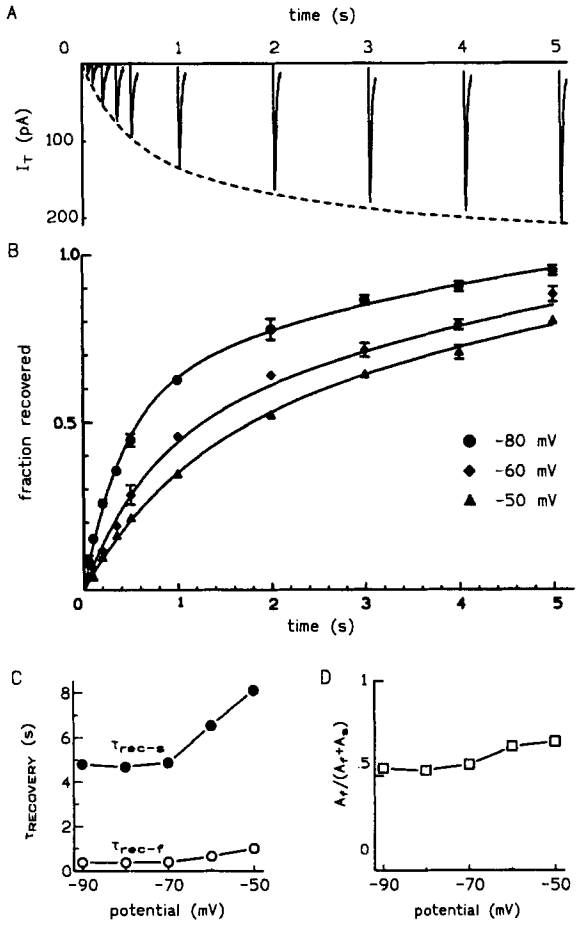

FIGURE 7. Voltage-dependent recovery kinetics of T current after inactivation. Time-dependent recovery of T Ca^{2+} current (inactivated by a 30-s prepulse to −20 mV) was monitored by applying voltage steps to 0 mV after stepping to one of five recovery potentials for periods ranging from 0.05 to 10 s. (*A*) Current records illustrating kinetics of recovery of T current at a repolarization potential of −80 mV. (*B*) Recovery curves; peak current amplitudes normalized to maximum current (fraction recovered) are plotted against time at recovery potentials of −50, −60, and −80 mV. Values are mean ± SEM (n = 4). Data points were fit with double exponential functions to obtain fast (τ_{rec-f}) and slow (τ_{rec-s}) time constants. (*C*) Fast and slow time constants plotted against recovery potential. (*D*) Fraction of Ca^{2+} current recovering with fast kinetics is plotted against recovery voltage for the same four cells as in *B* and *C*.

T-type Ca^{2+} channels in many cell types are distinctive in their relative insensitivity to toxins and organic Ca^{2+} channel modulators which potently affect other Ca^{2+} channel subtypes. ω-Conotoxin (fraction GVIA), a peptide from the venom of *Conus geographicus*, preferentially blocks neuronal-specific N-type Ca^{2+} channels. At a concentration of 1 μM, ω-conotoxin had no effect on the low voltage–activated Ca^{2+} current in adrenal cells (n = 3) (Fig. 9*A*).

The pure DHP Ca^{2+} agonist (−)Bay K 8644, which enhances Ca^{2+} current through L-type channels, did not have any significant effect on the T-type Ca^{2+} current of adrenal cells (data not shown). In two atypical cells where a high threshold, slowly inactivating Ca^{2+} current was present, (−)Bay K 8644 enhanced the magnitude of the current, shifted its voltage dependence, and slowed deactivation kinetics. Each of these responses is a characteristic feature of L current modulation by this agent (data not shown).

The expression of only T-type Ca^{2+} channels by a secretory cell is quite unusual. Further, L-type Ca^{2+} channels are functionally dependent on metabolic factors present in the cytoplasm and consequently L current rapidly "runs down" upon

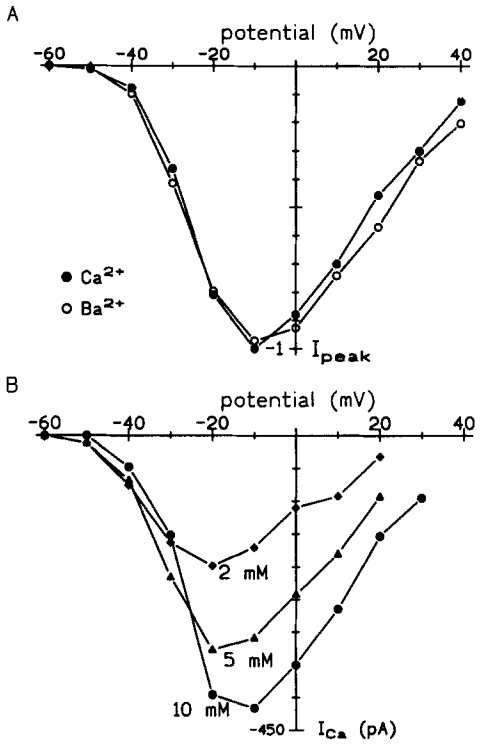

FIGURE 8. T currents in Ca^{2+} and Ba^{2+}. (*A*) Normalized average IV relationships obtained from seven cells with Ca^{2+} and Ba^{2+} as the charge carrier. Test potentials of varying size were applied at 20-s intervals from a holding potential of −80 mV in 10 mM Ca^{2+} and after switching the external solution to 10 mM Ba^{2+}. (*B*) IV relationships from a single cell at three different Ca^{2+} concentrations. Cell 1O25#3.

dilution of cell contents with pipette solution. In particular, phosphorylation by cAMP-dependent protein kinase may be an essential requirement. Including factors in the pipette or external medium which would facilitate phosphorylation has been shown to prevent rapid rundown or induce functional L-type channels (Cota, 1986; Armstrong and Eckert, 1987; Hille, 1992). We attempted to induce functional L-type Ca^{2+} channels in AZF cells by measures that would be expected to increase cAMP-dependent phosphorylation. Superfusion of cells with 100 μM 8-para-chlorophenylthio-cAMP did not induce an L-type current or change the T-type Ca^{2+} current in any of four cells tested. Forskolin (2.5 μM) was also ineffective in this respect. Pretreatment of adrenal cells for 1–3 h with either 100 μM 8-parachloro-

phenylthio-cAMP (n = 5) or 500 μM of the phosphodiesterase inhibitor isobutylmethylxanthine (n = 4) also failed to alter the characteristics of Ca^{2+} currents in these cells (data not shown). Apparently, the great majority of bovine AZF cells do not express either functional or dormant L-type Ca^{2+} channels.

T-type Ca^{2+} channels constitute the primary pathway for voltage-gated Ca^{2+} entry into bovine AZF cells. ACTH (1–24) at a concentration of 1 nM had no effect on the amplitude of T-type current (n = 3). However, this peptide strongly depolarizes AZF cells (Mlinar, Biagi, and Enyeart, 1993). To determine whether these Ca^{2+} channels

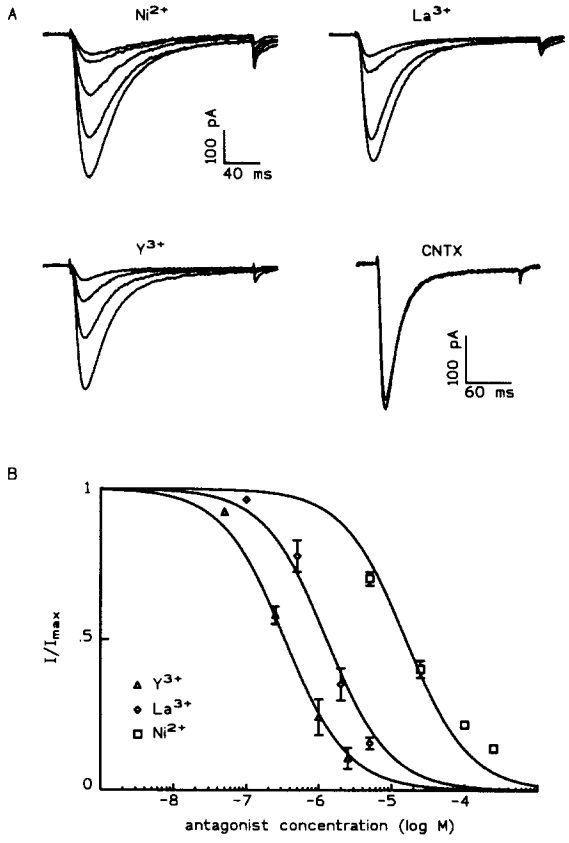

FIGURE 9. Pharmacology of T-type Ca^{2+} channels. Ca^{2+} currents were activated by voltage steps applied at 20-s intervals from a holding potential of −80 mV to a test potential of 0 mV. (*A*) Current records showing steady-state block by Ni^{2+} (5 and 25 μM), La^{3+} (0.5, 2, and 5 μM), Y^{3+} (0.25, 1, and 2.5 μM), and ω-conotoxin (*CNTX*). (*B*) Inhibition curves obtained from experiments as described in *A*. For each agent, normalized current is plotted as a function of antagonist concentration. Results are mean ± SEM of three to four determinations. Inhibition curves were generated by fitting data with an equation of the form $I/I_{max} = 1/(1 + [B/K_d])$, where B is antagonist concentration and K_d is the equilibrium dissociation constant.

are involved in cortisol secretion, we tested the effect of Ni^{2+} on ACTH-stimulated cortisol secretion by cultured cells. ACTH produced large (50–100-fold) increases in cortisol production which were inhibited by Ni^{2+} at concentrations similar to those that blocked T-type current (IC_{50} = 40 μM; data not shown).

DISCUSSION

In whole cell patch clamp recordings, bovine AZF cells were found to express primarily or exclusively a low voltage–activated, rapidly inactivating Ca^{2+} current.

This current has some biophysical and pharmacological properties resembling T-type Ca^{2+} currents previously described in other cells. Expression of this single Ca^{2+} channel subtype is a distinctive feature of these adrenal cells. Most secretory cells including neurons and endocrine cells express multiple Ca^{2+} channel subtypes as well as voltage-gated Na^{+} channels. The Ca^{2+} currents that we have described in AZF cells differ from those found in freshly dissociated cells of the bovine adrenal zona glomerulosa, where small (<30 pA) T- and L-type Ca^{2+} currents were observed in whole cell patch clamp recordings with 20 mM Ba^{2+} as the charge carrier (Cohen, McCarthy, Barrett, and Rasmussen, 1988). T-type Ca^{2+} currents were typically 10-fold larger in bovine AZF cells. Measurable L-type current was present in <3% of 86 cells tested. It isn't clear whether the differences in the magnitude of Ca^{2+} current between the two cell types are real or result from differences in cell isolation procedures. Regardless, our results indicate that T-type Ca^{2+} channels are the predominant pathway for voltage-gated Ca^{2+} entry into AZF cells.

Voltage Dependence of Gating

With regard to biophysical properties and pharmacology, the low voltage–activated Ca^{2+} channels of bovine AZF cells resemble, to some extent, T-type Ca^{2+} channels described in other cells. However, among T-type Ca^{2+} channels, sufficient variability has been documented to suggest the existence of various T channel subtypes. With respect to voltage-dependent gating, half-maximal activation has been reported to occur at potentials ranging from −61 to −17 mV, while half-maximal inactivation occurs over a voltage range of −113 to approximately −50 mV (Crunelli, Lightowler, and Pollard, 1989; Lorrand, Mironneau, and Pacaud, 1989; Mogul and Fox, 1992). In this regard, T current in AZF cells activates and inactivates at potentials more positive than those reported in nearly any cell. Although the voltage-dependent properties of T channels are not strictly tissue dependent, neuronal T channels gate at voltages that are on the average more negative than those in other tissues (Akaike, Kostyuk, and Osipchuk, 1989*b*; Coulter, Huguenard, and Prince, 1989; Crunelli et al., 1989; Mogul and Fox, 1992). Some of the voltage shifts may reflect differences in external divalent cation concentrations in various studies.

The slope of the activation curve for T channels was steeply voltage dependent and best fit by a Boltzmann function raised to an integer power of at least 4. Although this type of fit is consistent with a scheme wherein the opening of a T-type Ca^{2+} channel is associated with the movement of four independent voltage sensors, sequential gating models may fit the data equally well. In sequential models, the integer 4 would be regarded as indicative of a like number of conformational states of a single channel protein. In a previous study on thalamic relay neurons, voltage-dependent activation of T-type Ca^{2+} channels was modeled by a Boltzmann function raised to the third power (Coulter et al., 1989). A second power Boltzmann function has been used to describe the activation of T channels in bovine glomerulosa (Cohen et al., 1988).

Our estimate of single channel gating charge, obtained from the Boltzmann fit of our activation curve, suggested that the opening of a single T-type Ca^{2+} channels is associated with the movement of 8.1 elementary charges through the entire electric field of the membrane. A second estimate of 6.8 elementary charges obtained from

the limiting logarithmic potential sensitivity may be more satisfactory since it provides a model-independent estimate of the equivalent gating charge. This limiting steepness reflects the total charge moved as the channels travel to the open state from the particular closed state that predominates at negative potentials. Exploration of even more negative potentials could provide a larger value of q. Estimates of single channel gating charge for T-type Ca^{2+} channels range from 2.5 to 10.4 elementary charges. This indicates considerable variability in the steepness with which low threshold Ca^{2+} conductance depends on membrane potential in various cells (Cohen et al., 1988; Hagiwara, Irisawa, and Kameyama, 1988; Coulter et al., 1989; Crunelli et al., 1989).

Gating Kinetics

The sigmoidal onset kinetics fit by an exponential raised to the fourth power suggests that multiple voltage-dependent transitions are associated with the opening of individual Ca^{2+} channels in these cells. Delayed onset kinetics of Ca^{2+} channels have been observed in many cell types and described by first-order processes raised to integer powers ranging from 1 to 6 (reviewed by Hagiwara and Byerly, 1981). The wide range of values undoubtedly reflects the multiple varieties of Ca^{2+} channels present in various cells. Activation of T-type Ca^{2+} channels in thalamocortical relay neurons has been described by m^3h kinetics (Coulter et al., 1989).

Measurement of kinetic properties of AZF T-type Ca^{2+} current over a wide range of potentials indicated the presence of both voltage-dependent and -independent transitions as channels move among closed, open, and inactivated states. Activation kinetics were clearly voltage dependent but τ_a approached a voltage-independent minimum value with strong depolarizations. We interpret this result to mean that both voltage-dependent and -independent steps must be traversed on the path from the resting to the open state. At extreme potentials, the voltage-dependent transitions are relatively fast, and voltage-independent transitions become rate limiting. Thus, the minimum value for τ_a of 1.6 ms strongly suggests that an intrinsically voltage-independent transition with a rate constant of $\sim$625/s determines a maximum rate of T channel opening. Maximum rates for T current activation have been observed at test potentials near 0 mV in other cell types (Akaike, Kanaide, Kuga, Nakamura, Sadoshima, and Tomoike, 1989*a*; Akaike et al., 1989*b*).

The voltage-dependent inactivation kinetics of AZF T-type Ca^{2+} current resembled those of other cells where τ_i decreases progressively with stronger depolarizations toward an apparent minimum value (Akaike et al., 1989*a*, *b*; Coulter et al., 1989; Crunelli et al., 1989; Biagi and Enyeart, 1991; Chen and Hess, 1990). This value of $\sim$18 ms observed at test potentials from 0 to +40 mV indicates that an intrinsically voltage-independent rate constant, with an estimated value of 55 s^{-1}, limits the maximum inactivation rate. Apparently, as suggested for T-type Ca^{2+} channels in fibroblasts (Chen and Hess, 1990), macroscopic inactivation in AZF cells depends on membrane potential only when the voltage-dependent process of activation is rate limiting. In quantitative terms, τ_i reaches a minimum value of $\sim$20 ms for T channels in many cell types (Akaike et al., 1989*a*; Coulter et al., 1989; Crunelli et al., 1989; Biagi and Enyeart, 1991), while T channels in fibroblasts and some other cells inactivate more rapidly (Hagiwara et al., 1988; Chen and Hess, 1990).

The slow and voltage-dependent deactivation kinetics of T-type Ca^{2+} channels in AZF cells are characteristic features of these channels in all cell types studied so far. The τ_d of ~2 ms observed at a repolarization potential of −80 mV is comparable to τ_d's observed in other cells, where values ranging from 1.5 to 3.4 ms have been reported at the same voltage (Matteson and Armstrong, 1986; Hagiwara et al., 1988; Biagi and Enyeart, 1991). Although T channel closing rates in various cells are enhanced with increasingly negative holding potentials, only one previous study used extreme repolarization voltages to uncover a rate-limiting, voltage-independent transition during channel closing. In this study on fibroblasts, a voltage-independent τ_d of <1 ms has been observed by examining deactivation kinetics at potentials as negative as −180 mV (Chen and Hess, 1990). In our study τ_d decreased exponentially over potentials from −40 to −150 mV and also appeared to reach a voltage-independent minimum value.

Recovery from inactivation occurred with two voltage-dependent time constants, both of which reached minimum values at potentials of approximately −80 mV. These data are consistent with the presence of two inactivated states. Pathways from each of these leading to the closed state must include one voltage-independent transition which becomes rate limiting at very negative potentials. Considerable variability exists among T currents in excitable cells with respect to voltage-dependent recovery kinetics. In some cells, recovery occurs with a single time constant that approaches a clear minimum value at negative potentials, while in other cells no minimum value of τ_r is observed (Carbone and Lux, 1987; Akaike et al., 1989*b*; Chen and Hess, 1990). In different cells where recovery occurs along a single exponential, τ_r has also been reported to vary ~10-fold, ranging from hundreds of milliseconds (Hagiwara et al., 1988; Peres, Sturani, and Zippel, 1988; Coulter et al., 1989; Chen and Hess, 1990) to several seconds (Carbone and Lux, 1987; Akaike et al., 1989*b*; Biagi and Enyeart, 1991). Biphasic voltage-dependent recovery kinetics with comparable fast and slow time constants have been observed for channels only in vascular smooth muscle and rat sensory neurons (Bossu and Feltz, 1986; Akaike et al., 1989*a*). The rate of recovery of inactivated T channels may set a limit on voltage-gated Ca^{2+} entry and associated cortisol secretion by AZF cells.

Pharmacology

Pharmacologically, T-type Ca^{2+} channels in AZF cells resemble, in many respects, low threshold Ca^{2+} channels in other cell types. In response to inorganic antagonists, they were blocked by Ni^{2+} half-maximally at a concentration of 20 μM, while the trivalent elements La^{3+} and Y^{3+} were 15 and 80 times more potent. Previously, we had observed this same relative order of potency in other endocrine cells (Biagi and Enyeart, 1990, 1991).

The absence of L-type channel Ca^{2+} current in our recordings was a point of concern since secretion studies involving DHP Ca^{2+} channel modulators in bovine AZF cells suggested that L channels were present and could function in regulating cortisol secretion (Yanagibashi et al., 1990). Our attempts to expose dormant L-type Ca^{2+} channels that may have become nonfunctional during the cell isolation procedure or washed out during whole-cell patch clamping were unsuccessful. In other cells, agents that maintain or enhance phosphorylation capacity prevent

"rundown" or enhance current through L-type Ca^{2+} channels (see Hille, 1992), chapter 7, for review). These agents did not uncover L-type Ca^{2+} channels in our patch clamp experiments. It is likely that previously reported effects of DHP antagonists on cortisol secretion by bovine AZF cells result from interaction with T-type Ca^{2+} channels in these cells (Enyeart, Mlinar, Enyeart, and Biagi, 1992).

Role in Cortisol Secretion

The function of T-type Ca^{2+} channels in bovine AZF cell electrical activity and cortisol secretion is not well understood. Most secretory cells that possess T current generate action potentials supported by voltage-gated Na^+ current and we have not observed spontaneous action potentials in intracellular recordings from >50 cells at 37°C (Milnar, B., B.A. Biagi, and J.J. Enyeart, unpublished observations). Thus, we have no evidence that T-type Ca^{2+} channels regulate action potential generation in bovine AZF cells. In rat adrenal fasciculata and glomerulosa cells, stimulated Ca^{2+}-dependent regenerative electrical responses have been observed under conditions where outward currents are blocked (Quinn, Cornwall, and Williams, 1987). It isn't known whether these cells generate action potentials under physiological conditions.

Whether or not bovine AZF cells generate action potentials, our finding that Ni^{2+} blocked ACTH-stimulated cortisol secretion and T-type Ca^{2+} current with similar potency indicates that Ca^{2+} entry through these channels may be an important physiological stimulus regulating steroidogenesis. Recent studies using a variety of organic Ca^{2+} antagonists are consistent with this interpretation (Enyeart et al., 1992). In this regard, we have discovered that ACTH at subnanomolar concentrations strongly depolarizes bovine AZF cells (Mlinar et al., 1992). We propose that T-type Ca^{2+} channels, as the primary pathway for voltage-gated Ca^{2+} entry in bovine AZF cells, function critically in coupling membrane depolarization to cortisol synthesis and secretion.

This work was supported by National Institute for Diabetes and Digestive and Kidney Disorders grant DK-40131 to J. J. Enyeart.

Original version received 17 August 1992 and accepted version received 13 April 1993.

REFERENCES

Akaike, N., H. Kanaide, T. Kuga, M. Nakamura, J.-I. Sadoshima, and H. Tomoike. 1989*a*. Low-voltage-activated calcium current in rat aorta smooth muscle cells in primary culture. *Journal of Physiology.* 416:141–160.

Akaike, N., P. G. Kostyuk, and Y. V. Osipchuk. 1989*b*. Dihydropyridine-sensitive low-threshold calcium channels in isolated rat hypothalamic neurons. *Journal of Physiology.* 412:181–195.

Armstrong, C. M., and D. R. Matteson. 1985. Two distinct populations of calcium channels in a clonal line of pituitary cells. *Science.* 227:65–67.

Armstrong, D., and R. Eckert. 1987. Voltage-activated calcium channels that must be phosphorylated to respond to membrane depolarization. *Proceedings of the National Academy of Sciences, USA.* 84:2518–2522.

Bean, B. P. 1989. Classes of calcium channels in vertebrate cells. *Annual Review of Physiology.* 51:367–384.

Biagi, B. A., and J. J. Enyeart. 1990. Gadolinium blocks low- and high-threshold calcium currents in pituitary cells. *American Journal of Physiology.* 259:C515–C520.

Biagi, B. A., and J. J. Enyeart. 1991. Multiple calcium currents in a thyroid C-cell line: biophysical properties and pharmacology. *American Journal of Physiology.* 260:C1253–C1263.

Bondy, P. K. 1985. Williams Textbook of Endocrinology. W.B. Saunders Company, Philadelphia. 489–620.

Bossu, J.-L., and A. Feltz. 1986. Inactivation of the low threshold transient calcium current in rat sensory neurons: evidence for a dual process. *Journal of Physiology.* 376:357–391.

Carbone, E., and H. D. Lux. 1987. Kinetics and selectivity of a low-voltage-activated calcium current in chick and rat sensory neurones. *Journal of Physiology.* 386:547–570.

Chen, C., and P. Hess. 1990. Mechanisms of gating of T-type calcium channels. *Journal of General Physiology.* 96:603–630.

Cohen, C. J., and R. T. McCarthy. 1987. Nimodipine block of calcium channels in rat anterior pituitary cells. *Journal of Physiology.* 387:195–225.

Cohen, C. J., R. T. McCarthy, P. Q. Barrett, and H. Rasmussen. 1988. Ca channels in adrenal glomerulosa cells: K^+ and angiotensin II increase T-type Ca channel current. *Proceedings of the National Academy of Sciences, USA.* 85:2412–2416.

Cota, G. 1986. Calcium channel currents in pars intermedia cells of the rat pituitary gland. Kinetic properties and washout during intracellular dialysis. *Journal of General Physiology.* 88:83–105.

Coulter, D. A., J. R. Huguenard, and D. A. Prince. 1989. Calcium currents in rat thalamocortical relay neurons: kinetic properties of the transient, low-threshold current. *Journal of Physiology.* 414:587–604.

Crunelli, V., S. Lightowler, and C. E. Pollard. 1989. A T-type calcium current underlies low threshold potentials in cells of the cat and rat lateral geniculate nucleus. *Journal of Physiology.* 413:543–561.

Durroux, T., N. Gallo-Payet, and M. D. Payet. 1988. Three components of the calcium current in cultured glomerulosa cells from the rat adrenal gland. *Journal of Physiology.* 404:713–729.

Enyeart, J. J., B. A. Biagi, R. N. Day, S. S. Sheu, and R. A. Mauer. 1990. Blockade of low and high threshold Ca^{2+} channels by diphenylbutylpiperidine antipsychotics linked to inhibition of prolactin gene expression. *Journal of Biological Chemistry.* 265:16373–16379.

Enyeart, J. J., B. Mlinar, J. A. Enyeart, and B. A. Biagi. 1992. A dihydropyridine-sensitive T-type calcium current required for adrenocorticotrophic (ACTH)-stimulated cortisol secretion. *Society for Neuroscience Abstracts.* 18:188.11.(Abstr.)

Fenwick, E. M., A. Marty, and E. Neher. 1982. Sodium and calcium channels in adrenal chromaffin cells. *Journal of Physiology.* 331:599–635.

Goldman, D. E. 1943. Potential, impedance and rectification in membranes. *Journal of General Physiology.* 27:37–60.

Gospodarowicz, D., C. R. Ill, P. J. Hornsby, and G. N. Gill. 1977. Control of bovine adrenal cortical cell proliferation by fibroblast growth factor: lack of effect of epidermal growth factor. *Endocrinology.* 100:1080–1089.

Hagiwara, N., H. Irisawa, and M. Kameyama. 1988. Contribution of two types of calcium currents to the pacemaker potentials of rabbit sino-atrial node cells. *Journal of Physiology.* 395:233–253.

Hagiwara, S., and L. Byerly. 1981. Calcium channel. *Annual Review of Neuroscience.* 4:69–125.

Hamill, O. P., A. Marty, E. Neher, B. Sakmann, and F. J. Sigworth. 1981. Improved patch clamp techniques for high resolution current recording from cells and cell-free membrane patches. *Pflügers Archiv.* 398:284–297.

Hess, P. 1990. Calcium channels in vertebrate cells. *Annual Review of Neuroscience.* 13:337–356.

Hille, B. 1992. Ionic Channels of Excitable Membranes. Sinauer Associates, Inc., Sunderland, MA. 607 pp.

Hodgkin, A. L., and B. Katz. 1949. The effect of sodium ions on the electrical activity of the giant axon of the squid. *Journal of Physiology.* 108:37–77.

Lorrand, G., C. Mironneau, J. Mironneau, and P. Pacaud. 1989. Two types of calcium currents in single smooth muscle cells from portal vein. *Journal of Physiology.* 412:338–349.

Matsunaga, H., Y. Maruyama, I. Kojima, and T. Hoshi. 1987. Transient Ca^{2+}-channel current characterized by a low-threshold voltage in zona glomerulosa cells of rat adrenal cortex. *Pflügers Archiv.* 408:351–355.

Matteson, D. R., and C. M. Armstrong. 1986. Properties of two types of calcium channels in clonal pituitary cells. *Journal of General Physiology.* 87:161–182.

Mlinar, B., B. A. Biagi, and J. J. Enyeart. 1993. A novel K^+ current inhibited by ACTH and Angiotensin II in adrenal cortical cells. *Journal of Biological Chemistry.* 268:8640–8644.

Mogul, D. J., and A. P. Fox. 1992. Characterization of Ca^{2+} channels in acutely isolated hippocampal CA# pyramidal neurons: evidence for multiple types of Ca^{2+} channels. *Journal of Physiology.* 433:259–281.

Peres, A., E. Sturani, and R. Zippel. 1988. Properties of the voltage-dependent calcium channel of mouse Swiss 3T3 fibroblasts. *Journal of Physiology.* 401:639–655.

Quinn, S. J., M. C. Cornwall, and G. H. Williams. 1987. Electrical properties of isolated rat adrenal glomerulosa and fasciculata cells. *Endocrinology.* 120:903–914.

Schoppa, N. E., K. McCormack, M. A. Tanoute, and F. Sigworth. 1992. The size of gating charge in wild-type and mutant *Shaker* potassium channels. *Science.* 255:1712–1715.

Suzuki, S., and M. A. Rogawski. 1989. T-type calcium channels mediate the transition between tonic and phasic firing in thalamic neurons. *Proceedings of the National Academy Sciences, USA.* 86:7228–7232.

Wang, X.-J., J. Rinzel, and M. A. Rogawski. 1991. A model of the T-type calcium current and the low-threshold spike in thalamic neurons. *Journal of Neurophysiology.* 66:839–850.

Yanagibashi, K., M. Kawamura, and P. F. Hall. 1990. Voltage-dependent Ca^{2+} channels are involved in regulation of steroid synthesis by bovine but not rat fasciculata cells. *Endocrinology.* 126:311–318.